CHAPTER 2

Background

2.1 Nanomaterials

Nanomaterials are materials with morphology in range of one to hundreds in nanometer (10^{-9}m.)as shown in Figure 2.1. A unique aspect of nanomaterials is the widely increased ratio of surface to volume which reveals new quantum effects. Materials denoted to the nanoscale can exhibit extremely different feature compared with a macroscale and bulk materials.

Nanomaterials are normally grouped by their dimensionalities as zero dimensional (dots or nanoparticles[29]), one dimensional (nanowires[13], nanotubes[30], and nanorod[31]) or two dimensional (thin films). These types point to the number of dimensions in which of the material is outside the nano regime. Materials which are nanoscaled in all three dimensions are determined 0D nanomaterials. These include thin films deposited under conditions that originate atomic-scale porosity, colloids, and free nanoparticles with various morphologies. One dimensional (1D) nanomaterials have two dimensions in the nanometer scale, *i.e.* its width and thickness are between 0.1 and 100 nm whereas its length could be much greater. Free particles with a large aspect ratio, with dimensions in the nanoscale range, are also considered one nanomaterials (1D), *i.e.* nanobelts, nanorods, nanotubes and nanofibers are all examples of 1D nanostructures. These also include 1D nanostructured films, with nanostructures firmly attached to a substrate, or nanopore filters used for small particle separation and filtration. A thin film consists of large expanses of material in both in-plane directions, and is nano regime only in its thickness: therefore it is termed a two dimensional (2D) nanomaterials.

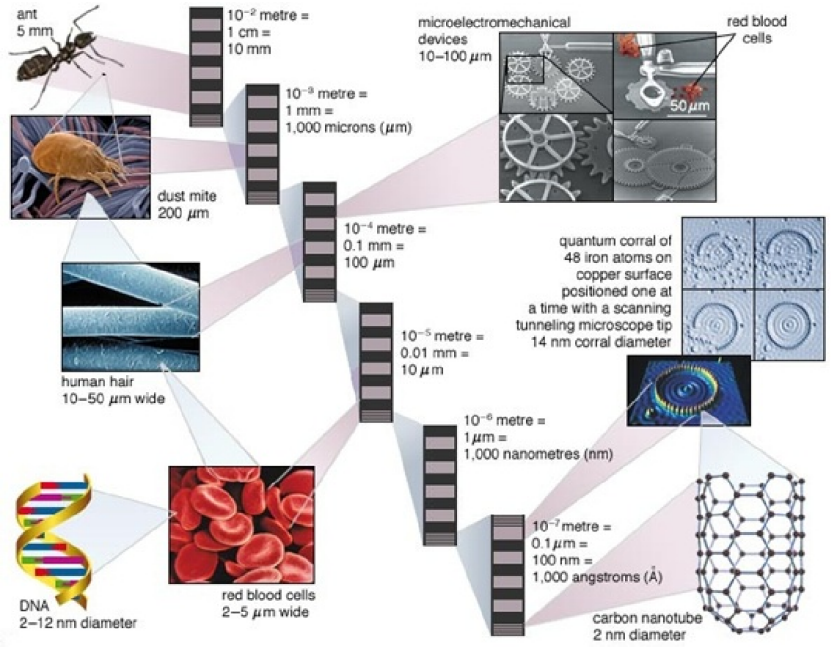

Figure 2.1: Scale from micrometer to nanometer dimensions. (Encyclopaedia Britannica, Inc.)

2.2 Quantum effect[32]

The quantum effect in nanomaterials, is also known as quantum limitation. It occurs due to the changes in the atomic structure. Since, the mechanical, electrical, optical and magnetic properties of materials depend influentially on how the energies are distributed hence the small length scale is the direct influence on the energy band structure. In aspect of the fact, band structure in metal or semiconductor is a group of atomic orbital. Each of N atoms conduces to its atomic states to a band so that the density of states (DOS) within a band is basically proportional to the number of atoms of an ensemble with spread the band-like state. To estimate these properties, It needs to consider the DOS. That define the number of free particles having an energy of E as $N(E)$. The density of states is then defined as

$$D(E) = \frac{d}{dE}N(E) \tag{2.1}$$

We have used parabolic energy dispersion to show one example of 3 dimentional nanostructureas followed

$$E_n = \frac{\hbar^2 k_n^2}{2\mathrm{m}} \tag{2.2}$$

Then cubic *k*-state distribution, is given by

$$k^2 = \frac{3\pi^2 N(k)}{V} \tag{2.3}$$

Thus, it can be written

$$N = \frac{V}{3\pi^2}\left(\frac{2\mathrm{m}E_n}{\hbar^2}\right)^{\frac{3}{2}}$$

or

$$N(3D) = \frac{2 \times (volume)_{k-space}}{\left(\frac{2\pi}{L}\right)^3_{state-spacing}}$$

$$N(3D) = \frac{2 \times 4\frac{\pi k_n^3}{3}}{\left(\frac{2\pi}{L}\right)^3}$$

$$N(3D) = \frac{V}{3\pi^2}k_n^3 \tag{2.4}$$

From Eq. (2.4), Eq. (2.1) can be written as

$$D(E) = \frac{dN(3D)}{dE} = \frac{V}{(2\pi^2)}\left(\frac{2\mathrm{m}}{\hbar^2}\right)^{\frac{3}{2}} E^{\frac{1}{2}}$$

$$D(E) \propto \sqrt{E} \tag{2.5}$$

For 2D and 1D, the density takes into account of higher lying subbands. For 0D, a spectrum of $D(E)$ functions is expected. The density of states formulas $D(E)$ for these four case is listed below:

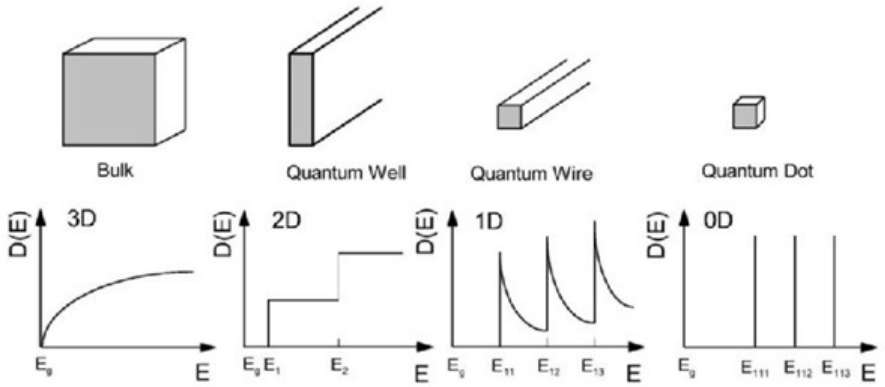

Figure 2.2: The density of states D(E) of various nanostructures[54]

3 dimentional limitation : $D\left(E\right) \propto \sqrt{E}$

2 dimentional limitation : $D\left(E\right) \propto constant$

1 dimentional limitation : $D\left(E\right) \propto \frac{1}{\sqrt{E-E_N}}$

0 dimentional limitation : $D(E) \propto \delta(E - E_N)$,

where $D\left(E\right)$is densty of state representation, and E_N is the energy at N level.

2.3 Zinc oxide

ZnO is a wide-band-gap semiconductor with a direct band-gap of 3.37 eV[33]. It is amorphous in color of white or yellow. But it is generally known as white powder. The white color of ZnO appears as a mineral called zincite. The mineral composes of manganese and some other elements. Therefore, this mineral is yellowish or red in color.

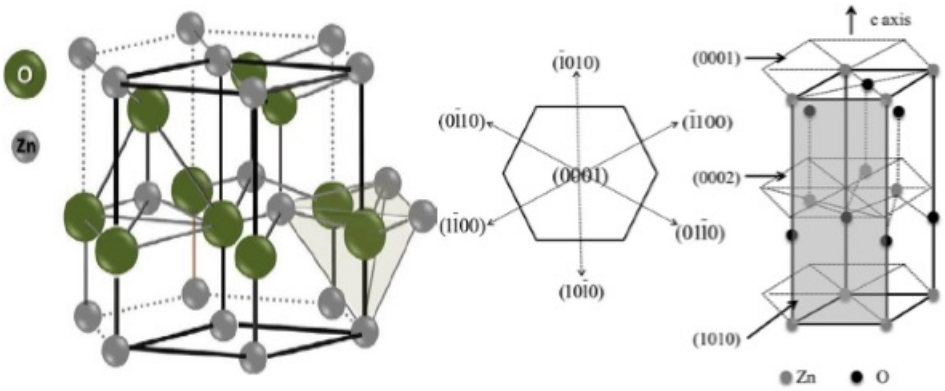

Figure 2.3: Hexagonal zinc-oxide structures and Miller index planes (Gul Amin,2012)

ZnO consists of three different crystal structures, i.e. hexagonal wurtzite, cubic zincblende, and the infrequently observed cubic rocksalt as shown in Figure 2.3. ZnO is thermodynamically stable in the wurtzite phase owning to the effect and the bonding class is precisely at the border between covalent and ionic. The lattice constants of wurtzite structure range from 3.2475 to 3.2501 angstrom for parameter a and from 5.2042 to 5.2075 angstrom for parameter c The c/a ratio[34] varies in a range, from 1.593 to 1.6035.

ZnO is a relatively soft material with approximate hardness of 4.5, having high heat conductivity and heat capacity, poorly thermal expansion and high melting temperature. It is beneficial for ceramics. Among the tetrahedrally bonded semiconductors, it has been stated that ZnO has high piezoelectric tensor. This property can be applied for many piezoelectrical technologies, which require a large electromechanical coupling. The general properties of ZnO are shown in Table 2.1

Table 2.1: General properties of ZnO

Properties	Volumes
Molecular weight	81.37
Average atomic weight	40.69
Average atomic number	19
Enthalpy of formation (298K)(kJ/mol)	-350.5
Coefficient of thermal expansion : Along the c-axis (1/K)	2.9×10^{-6}
Coefficient of thermal expansion : Across the c-axis (1/K)	4.8×10^{-6}
Density $\left(\mathrm{g/m^3}\right)$	5.6803
Melting point (K)	$2,248$

2.4 Zinc oxide nanowires

ZnO nanostructures can be synthesized into a category of morphologies along with whisker, nanobelt, nanowires and nanorods. Interestingly, ZnO nanowires are good candidate to be applied in gas sensor technology. ZnO can be prepared in various technique such as electrospun[33], puled laser deposition[23], and thermal oxidation technique[35,36]. Through the methods above, the size of nanostructure is distributed between ten to hundreds of nanometers. Alternatively, Chemical vapor deposition (CVD) is a good technique to grow nanowires of zinc oxide semiconductors[28,37]. The ZnO nanowires will be uniform in size and high quality cystal structure. Advantage of ZnO nanowires has displayed nontoxicity, chemical stability, electrochemical activity, and good sensing properties due to high surface to volume ratio.

2.5 Chemical vapor deposition technique

One of the most popular thin-film deposition technologies being employed is chemical vapor deposition (CVD) technique due to its capability to grant uniform surface deposition. In the process, high temperature decomposes chemical vapor precursor. The material will be deposited on the surface when the vapor comes into contact with heated substrate surface. The CVD mechanism can be separated to five considerable steps. The first and second step include diffusing the reactants to the substrate and adsorbing onto the surface. The third obliges the surface chemical reactions leading to a deposition of the solid phase. Next, gaseous by products start a desorption process from the surface. Finally, gaseous by products begin to diffuse into the stream. CVD is normally fulfilled at high temperatures and may enclose erosive by products due to chemical reactions (see Figure 2.4).

CVD covers a several of reactor types which are decided based on the material substrate, coating, morphology, uniformity, and cost. Some process types include atmospheric pressure chemical vapor deposition (APCVD)[38], high-pressure chemical vapor deposition (LPCVD)[39], and plasma-enhanced chemical vapor deposition (PECVD)[31]. Among them, APCVD offers a very high deposition rate. However, it is low purity and

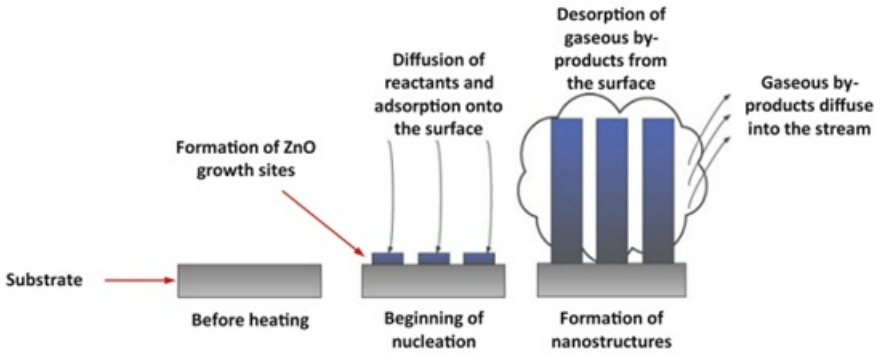

Figure 2.4: Chemical vapor deposition technique (Intech,2011)

poor uniformity owning to operate in normal atmospheric conditions. While LPCVD can be used to improve uniformity and purity but with higher temperatures and lower deposition rates than APCVD. Lastly, PECVD operates under low pressures and dispense thermal energy to activate the reaction process.

2.6 Growth mechanism of nanostructure

Nanostructures can be produced by chemical vapor deposition technique showing variety of shapes and morphologies. It is interestingly to understand the growth mechanism of nanostructures. Recently, there are many models to explain the growth mechanism of nanostructure such as vapor-solid phase (VS) mechanism and vapor–liquid–solid phase (VLS) mechanism.

2.6.1 Vapor-solid phase mechanism

Vapor–solid (VS) mechanism is in general applied for nanostructure growth in areas that gas phase condenses and deposits. Deposition occurs on the top that affects to increase in length of nanostructure. This process here is illustrated in Figure 2.5.

2.6.2 Vapor–liquid–solid phase mechanism

Vapor–liquid–solid (VLS) mechanism is in general used for nanostructure growth in areas seeded by the metal catalyst. Therefore, their diameters are mainly determined

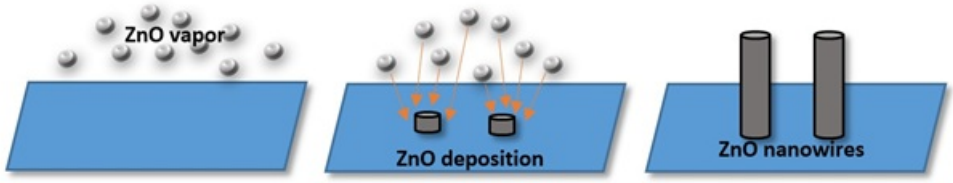

Figure 2.5: Mechanism of vapor-solid phase

by the size of the catalyst. In the case of nanowires, the VLS method uses nano-sized metal clusters as catalyst to absorb gas phase reactants and to form nuclei — as the reactants in the droplets become supersaturated, precipitation takes over and one dimensional nanowires begin to form[40]. This process is presented in Figure 2.6.

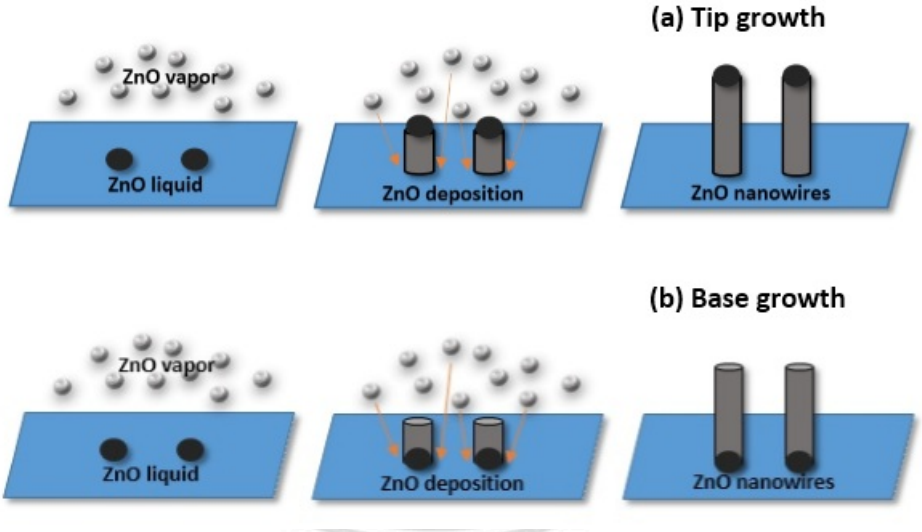

Figure 2.6: Mechanism of vapor-liquid-solid phase for (a) tip growth and (b) base growth

This technique usually involves growing ZnO nanowires on silicon (Si) or sapphire (Al_2O_3)substrates with the presence of a metal catalyst. Some popular catalysts include: gold (Au), silver (Ag), platinum (Pt), copper (Cu) and tin (Sn) . Moreover some metals have a self-catalyst properties such as Zn.

2.7 Growth mechanism of metal-oxide nanowire by thermal oxidation technique

The growth mechanisms of metal-oxide nanowires were considered based on the equation of nucleation probability which is in terms of temperature and surface energy. In

addition, diameter of metal-oxide nanowires will be controlled by temperature and supersaturation ratio as well[35].

2.7.1 Gibbs free energy change per volume (ΔG^0)

An important parameter to gain physical understanding into materials aspect of thermodynamics potential between product and precursor is Gibb free energy change per volume (called volume energy (ΔG^0) written by

$$\Delta G^0 = -RT \ln\left(\frac{P_{O_2(vapor)}}{P_{O_2(standard)}}\right) = -RT \ln(s), \tag{2.6}$$

where R is gas constant, T is temperature, s is supersaturation ratio, is ratio between partial pressure of oxygen in vapor phase and standard. It is the driving force for crystal nucleation and growth. Nucleation is the birth of new crystal nuclei – either spontaneously from primary nucleation or in the presence of existing crystals (secondary nucleation). This parameter represents phase transformation from precursor to be products that occur the two chemical reaction. While synthesis of metal-oxide nanowires in range of temperature from $400°C - 900°C$ is given by

$$M(s) + \frac{1}{2}O_2(g) \rightarrow MO(s) \tag{2.7}$$

and

$$M(l) + \frac{1}{2}O_2(g) \rightarrow MO(s), \tag{2.8}$$

where $M(s)$ and $M(l)$ defined metal in solid and liquid phase, respectively. The above equations as above show the two chemical reactions forming metal-oxide nuclei in thermal oxidation reactor. Eq.(2.7) and Eq.(2.8) represent oxidation reaction process below a melting point and above melting point, respectively.

2.7.2 Surface energy (σ)

Here, the surface energy (σ) for liquid phase will be presented. It is defined as the attractive forces that molecules in a liquid exert on one another at the bulk and surface

regions. At surface, this net attractive force causes the liquid surface to contract toward the interior until other repulsive external forces are exerted. This force is in terms of the surface tension and is defined as the force unit length (N/m)

Here, the surface energy for solid phase will be presented. It is defined as the energy of one bond for atoms in crystal through the concept of sublimation energy surface energy strongly depends on the crystal structure and also depends on the Miller index or sometimes called "facets"; low Miller index generally having low surface energy. The low-energy facets for various crystal structures are listed in the Table 2.2

Table 2.2: Facets of the lowest surface energy for various crystal structures (Smith,1995)

Structure	Example	Lowest facet
Body-centered cubic (bcc)	Cr, Fe	{110}
Face-centered cubic (fcc)	Au, Al	{111}
Hexagonal close-packed (hcp)	Zn, ZnO, Mg	{0001}
Diamond	Si, Ge	{111}
Rock salt	NaCl, PbTe	{100}

2.7.3 Gibbs free energy change per nuclei

In section 2.7.1, we discussed the Gibb free energy per volume (ΔG^0) as defined in Eq. (2.6), while the Gibb free energy per nuclei (ΔG_N) is differntly defined. J. Jemes[41] considered the dependence of the change in free energy during precipitation on the size of the nucleus. For simplicity, it is considered a spherical *homogeneous* nucleus of radius. The free energy change per nuclei (ΔG_N) is given by the *sum of* volume (ΔG_v) and *sum of* surface energy (ΔG_s) terms, namely;

$$\Delta G_N = \Delta G_v + \Delta G_s$$

$$\Delta G_N = -\left(\frac{4}{3}\pi r^3\right)\Delta G^0 + 4\pi r^2 \sigma_{homo}, \tag{2.9}$$

where r is radius, ΔG^0 is volume energy, and σ_{homo} is surface energy. The first term is negative and varies as the cube of r, while the second term is positive and varying as r^2. The sum of these two terms has a maximum that occurs when $\frac{d}{dr}(\Delta G_N) = 0$. This is

known as the critical radius r^*, which can be written as

$$r^*_{homo} = -\frac{2\sigma_{homo}}{\Delta G^0} \tag{2.10}$$

and

$$\Delta G^*_N = \frac{16\pi \left(\sigma^*_{homo}\right)^3}{3(\Delta G^0)^2}, \tag{2.11}$$

Moreover, the critical radius also implies the stability of nucleation. The nuclei will be stable at radius more than critical value r^* and proceed to grow up spontaneously. The same analysis can be performed for *heterogeneous* nucleation followed as

$$r^*_{heter} = -\frac{2\sigma_{heter}}{\Delta G^0} \tag{2.12}$$

and

$$\Delta G^*_N = \frac{16\pi \left(\sigma^*_{heter}\right)^3}{3(\Delta G^0)^2} \tag{2.13}$$

2.7.4 Nucleation probability (P_N)

The growth mechanism of nanostructures will be explained by nuclei probability. The critical size is that it controls the probability of a nucleus forming on any given timescale. The nucleation probability is proportional to the exponential of the barrier height (critical free energy change) divided by k_BT. Thus the nucleation rate is given by

$$P_N = exp(-\Delta G^*_N / k_BT) \tag{2.14}$$

2.8 Sensing property of ZnO nanowires

ZnO nanowires have been defined as wires with one dimension in the range up to 100 nm. This type of architectures exhibits a variety of interesting properties and has been functioning as building block for nanosensing technology. In spite of the basic, gas

sensing mechanism (adsorption and desorption gas) remains the same, compared to the conventional sensor based on thin film and microstructure. The ZnO nanowires gas sensors exhibit inspiring characteristic such as ultra-sensitivity and fast response time. Due to their small size with high surface to volume ratio, a few gas molecules are sufficient to change the electrical properties of the sensing elements. This allows the detection of a very low concentration of gas within some seconds.

The sensing mechanism is normally controlled by the absorbed gas (reducing/oxidizing gases), tripping or providing the electron on the sensor surface. Thus, the sensor resistance will be changed. When the ZnO nanostructure sensor was exposed under the target gas, ethanol (Ethanol : CH_3CH_2OH) for example, ethanol will react with adsorbed oxygen on surface and generate new gas molecules and other products. Then, the adsorbed oxygen on sensor surface will give up electrons back to sensor surface. Therefore, sensor resistance is changed; decrease for n-type metal-oxide semiconductor and increase for p-type metal-oxide semiconductor. As a result, the sensor sensitivity can be calculated by the change of the electron density which represented by sensitivity. Typically, electron density on surface under target gas (Ethanol : CH_3CH_2OH) will be represented by reaction rate equation as

$$\frac{dn}{dt} = k_{Eth}(T)\left[O_{ads}^{ion}\right]^b \left[CH_3CH_2OH\right]^b, \tag{2.15}$$

where *n* is the electron density or electron concentration under ethanol atmosphere, b is a charge parameter having of 1 for O^- and 0.5 for O^{2-} and $k_{Eth}(T)$ is the reaction rate constant or reaction rate coefficient, as given by

$$k_{Eth}(T) = A\exp(-\frac{E_a}{RT}), \tag{2.16}$$

where A is frequency factor, E_a is activation energy, R is gas constant (8.314 J/mol•K) and T is Kelvin temperature. Integrating Eq. (2.16) leads to the solution as

$$n = k_{Eth}(T)\left[O_{ads}^{ion}\right]^b \left[CH_3CH_2OH\right]^b t + n_0, \tag{2.17}$$

where n_0 represents the electron concentration of sensor at an operating temperature in the air atmosphere. At equilibrium under ethanol and air atmosphere carrier concentration, n and n_0 can be considered as a constant with time. Thus, Eq. (2.17) can be rewritten as

$$\frac{1}{R_g} = \frac{\Gamma_t k_{Eth}(T) \left[\mathrm{O}_{ads}^{ion}\right]^b \left[\mathrm{CH_3CH_2OH}\right]^b}{\alpha} + \frac{1}{R_a} \tag{2.18}$$

The gas response, S_g, of the sensor is defined as R_a/R_g ,where R_a and R_g is the electrical resistance of the sensor in air and in ethanol-air mixed gas, respectively. And Γ_t is defined as time constant. Therefore, the sensor response relation can be obtained as followed

$$S_g = \frac{R_a}{R_g} = \frac{\Gamma_t k_{Eth}(T) \left[\mathrm{O}_{ads}^{ion}\right]^b \left[\mathrm{CH_3CH_2OH}\right]^b}{n_0} \tag{2.19}$$

Usually, temperature dependence of sensor response is controlled by two parameters; reaction rate coefficient $k_{Eth}(T)$ between adsorbed oxygen ions with ethanol molecules and electron density of the sensor n_0. The reaction rate coefficient and electron density increase exponentially with increasing temperature. However, sensor response is proportional to reaction rate coefficient but inversely proportional to electron density. These two parameters compete with each other and result in maximum sensor response at optimum operating temperature. Ethanol gas sensor based on ZnO material has optimum operating temperature around 300°C[4].

Hongsith, N. *et al*. reported the general sensor response formula for ZnO nanostructures. This formula is in good agreement with experimental results and valid for the case of oxygen ion species, metal doping[42], nanostructure with diameter larger than L_d, and nanostructure with diameter of about L_d, where L_d is Debye length. Absorbed oxygen controlled the mechanism of sensor by trapping electron from the conduction band and then forming oxygen ions on sensor surface. This result increases the sensor resistance. While target gas is introduced, adsorbed oxygen will react with the target gas forming other gases. This reaction decreases the sensor resistance allowing the sensor conducted more electrons. The sensor formulas for those cases are shown below

$$S_g = aC_g^b + 1 \tag{2.20}$$

$$S_g = \frac{\Gamma_t k_{Eth}(T)\left[O_{ads}^{ion}\right]^b}{n_0} C_g^b + 1 \tag{2.21}$$

$$S_g = \frac{\Gamma_t k_{Eth}(T)\left[\sigma_0 \Phi(V_m/V_s)\right]^b}{n_0} C_g^b + 1 \tag{2.22}$$

$$S_g = \frac{\Gamma_t k_{Eth}(T)\left[\sigma_0 \Phi(V_m/V_s)\right]^b}{n_0} \left(\frac{D^2}{(D-2L_d)^2}\right) C_g^b + 1, \tag{2.23}$$

where a is a constant depending on types of test gases; sensing material; and operating temperature, C_g is a gas concentration and O_{ads}^{ion} is adsorbed oxygen species concentration which can be explained by

$$\mathrm{O}_{ads}^{ion} = \sigma_0 \Phi(V_m/V_s) \tag{2.24}$$

where σ_0 and Φ are number of oxygen ion per unit area and a ratio of surface area per volume of material (V_m), respectively, while V_s is the system volume. For Eq. (2.23), D is a diameter of sensing material. All formulas are valid for the case of oxygen ion species, Eq. (2.21) are valid for the case of metal doping, while nanostructures with L_d ($D \sim L_d$) can be explain by both Eq. (2.22) and (2.23). For nanostructures with $D \sim L_d$, the last formula is valid.

2.9 Sensitivity (S_g)

Sensitivity (S_g) is a change of measured signal per analytic concentration unit, i.e., the slope of calibration graph. The change of electrical properties of the metal-oxide semiconductor due to adsorption of gas molecule is primarily connected with the chemisorption of oxygen. Molecular oxygen adsorbs on the surface by trapping an electron from conduction band of the semiconductor. The general formula was given as;

$$S_g = \frac{R_a}{R_g} \tag{2.25}$$

where R_a is the resistance of sensor device under air and operating temperature and R_g is the resistance of sensor device under target gas and operating temperature.

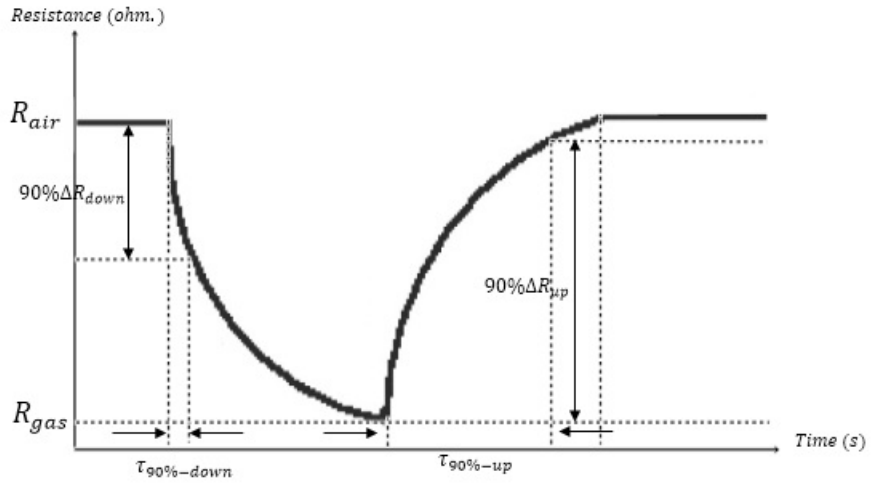

Figure 2.7: Plot of resistance as a function of time

2.9.1 Response time ($\tau_{90\%-down}$)

Response time is the time required for sensor to respond to a step concentration change from zero to a certain concentration value. For easily considering in some case that occurs the fluctuation of resistance. Response time will approximated by 90% of changing resistance.

2.9.2 Recovery time ($\tau_{90\%-up}$)

Recovery time is the time it takes for the sensor signal to return to its initial value after a step concentration change from a certain value to zero. In the same way, some case that happen of oscillating signal. Recovery time can simply calculated by 90% of changing resistance.